Journal of Low Temperature Physics, Vol. 107, Nos. 5/6, 1997

Hall-Array Measurements of Flux creep parameters in Y-Ba-Cu-O crystals

Y. Abulafia,[♮] A. Shaulov,[♮] Y. Wolfus,[♮] R. Prozorov,[♮] L. Burlachkov,[♮] D. Majer,[*] E. Zeldov,[*] V. M. Vinokur,[†] and Y. Yeshurun[♮]

[♮] *Institute of Superconductivity, Department of Physics, Bar-Ilan University, 52900 Ramat-Gan, Israel*

[*] *Department of Condensed Matter Physics, The Weizmann Institute of Science, Rehovot 76100, Israel*

[†] *Argonne National Laboratory, Argonne, IL 60439, USA*

We describe the details of a new method for studying thermally activated flux creep in superconductors. This method employs an array of microscopic Hall sensors to probe the time evolution of the field profile in the sample. We analyze these data on the basis of a continuity equation which takes into account contributions to the relaxation process from both *the in-plane and out-of-plane components of the induction field. This analysis enables direct determination of flux creep parameters such as the flux-line current density, flux-line velocity and the activation energy for flux creep. We demonstrate this method by presenting experimental data for* $YBa_2Cu_3O_{7-x}$ *crystals in the remanent state and in the presence of a field.*

PACS numbers: 74.60.Ge, 74.72.-h

1. INTRODUCTION

We have recently described a novel experimental approach[1,2] to determine the spatial and time dependence of flux creep parameters, such as the vortex velocity v, the flux current density D, and the activation energy U. In this technique we utilize an array of miniature Hall probes to measure the local induction B at different locations *simultaneously* as a function of time. In contrast with conventional techniques where the time evolution of

0022-2291/97/0600-0455$12.50/0

the *total* magnetization is recorded, we measure the time evolution of the *spatial distribution* of B, and thus are able to determine both the time and the spatial derivatives of B. Using this new information we analyze the local relaxation data on the basis of the continuity equation for the vortex lines.[3–5] This analysis allows a direct, model independent determination of the flux creep parameters.[1,2]

In this article we review our technique and discuss its details for the common geometry of platelet crystals. We also show data for the flux creep parameters in Y-Ba-Cu-O (YBCO) crystals, in the remanent state and in the presence of a field.

2. ANALYSIS

The differential equation governing flux creep in superconductors is derived[4] from the Maxwell equation $\nabla \times \mathbf{E} = -(1/c)\partial \mathbf{B}/\partial t$, and the equation relating the electric field $\mathbf{E}$ to the flux motion, $\mathbf{E} = (1/c)\mathbf{B} \times \mathbf{v}$, where $\mathbf{v}$ is the velocity of the vortices in the direction of the Lorentz force, $\mathbf{F}_L = (1/c)\mathbf{j} \times \mathbf{B}$. These equations lead to

$$\partial \mathbf{B}/\partial t = -\nabla \times (\mathbf{B} \times \mathbf{v}). \tag{1}$$

Assuming thermal activation over the pinning barrier $U(j)$, the magnitude of $\mathbf{v}$ is

$$v = v_0 \exp(-U/kT), \tag{2}$$

where $v_0 = \mathcal{A} j \phi_0 / c\eta$, ϕ_0 is the unit flux, c is the light velocity, j is the current density, η is the viscosity coefficient, and $\mathcal{A}$ is a numerical factor[1,6] of order 1.

For a slab geometry (infinite along the y and z directions with the magnetic field parallel to the z direction), $\mathbf{B} = (0, 0, B_z)$, $\mathbf{v} = (v, 0, 0)$ and Eq. (1) is reduced to the one dimensional continuity equation

$$\frac{\partial B_z}{\partial t} = -\frac{\partial D}{\partial x}, \tag{3}$$

where $D = B_z v$ is the vortex line current density. This one dimensional continuity equation has been used in many theoretical and experimental works,[1–5,7,8] involving different geometries, although it strictly applies to the case of infinite slab in a parallel field.

In reality samples have platelet shape and the field is applied perpendicular to their surface. In this case one should consider the component of $\mathbf{B}$ parallel to the surface as well. In the following we consider a rectangular sample of width $2w, (|x| \leq w)$, much smaller than its length (along the y direction). The Hall-probe array is placed in the middle of the sample,

perpendicular to its length (see Figure 1). We approximate the sample as an infinitely long strip with current of constant magnitude flowing along its length, $\mathbf{j} = (0, j{\cdot}sgn(x), 0)$. For such a strip in a perpendicular field (along z), $\mathbf{B} = (B_x, 0, B_z)$, $\mathbf{v} = (v_x, 0, v_z)$, and Eq. (1) yields:

$$\frac{\partial B_z}{\partial t} = -\frac{\partial}{\partial x}(B_z v_x - B_x v_z) \tag{4}$$

$$\frac{\partial B_x}{\partial t} = -\frac{\partial}{\partial z}(B_x v_z - B_z v_x). \tag{5}$$

These equations indicate that both components, B_z and B_x, exhibit relaxation, and that the relaxation of each component is *coupled* to that of the other. General analysis of the relaxation throughout such a sample requires the consideration of both components B_z and B_x which appear in equations (4) and (5). Obviously, analysis on the basis of either equation should lead to the same results as far as the flux creep parameters are concerned. Our Hall-probe array is sensitive to B_z; we therefore base our analysis on Eq. (4). Since $\mathbf{v} \cdot \mathbf{B} = 0$, for $B_z \neq 0$ Eq. (4) becomes

$$\frac{\partial B_z}{\partial t} = -\frac{\partial}{\partial x}\left(B_z v\sqrt{1+\delta}\right), \tag{6}$$

where $v = \sqrt{v_x^2 + v_z^2}$ and $\delta = B_x^2/B_z^2$. Equation (6) is formally equivalent to Eq. (3) if we define $D = B_z v\sqrt{1+\delta}$. The factor $\sqrt{1+\delta}$ may be considered as a correction factor accounting for the contribution of B_x to the relaxation process. As will be shown in the Appendix, this factor has a little effect on the relaxation in the presence of a field. Moreover, even in the remanent state one can define a significant area within the sample where this correction factor is close to 1. However, this factor becomes important in the vicinity of the so called 'neutral line'[9] in the remanent state where $B_z \to 0$. At this line both B_z and $\partial B_z/\partial t$ vanish, nevertheless $D = B_z v\sqrt{1+\delta}$ remains finite since $\sqrt{1+\delta} \to \infty$. For a constant j in the remanent state, $\sqrt{1+\delta}$ becomes a geometrical factor which can be calculated accurately and thus taken into account in the data analysis (see Appendix).

In the experiment we measure B_z as a function of x and t. The procedure of data analysis is as follows: We first integrate the measured values of $\partial B_z/\partial t$ to obtain $D = B_z v\sqrt{1+\delta}$. At this stage, *no approximation is made*, i.e. $D = cE_y$ is measured *accurately*.

Knowing $D(x,t)$ and B_z we then determine $v\sqrt{1+\delta}$ as the ratio D/B_z. In the presence of a field, or in the remanent state far from the neutral line, $\delta \approx 1$ (see Appendix), and this ratio yields the flux line velocity $v = v_0 \exp(-U/kT)$. To calculate v in the remanent state in the vicinity of the neutral line it is necessary to take into account the correction factor

$\sqrt{1+\delta}$, as outlined in the Appendix. Once v is known the activation energy $U(x,t)$ is derived by using Eq. (2):

$$U(x,t) = kT \ln\left(\frac{v_0}{v}\right). \tag{7}$$

We calculate v_0 using the relation $v_0 = \mathcal{A} j \phi_0 / c\eta$, where the flux viscosity coefficient $\eta(T)$ is taken from Golosovsky *et al.*[10] The current density j is derived by fitting the field profiles as described in the Appendix, and $\mathcal{A}$ is taken as 1. Thus, measurements of $B_z(x,t)$ allows a direct determination of $D(x,t)$, $v(x,t)$, and $U(x,t)$.

3. EXPERIMENTAL

Measurements were performed on two $YBa_2Cu_3O_7$ crystals[11,12] ($T_c \simeq 91\ K$), with rectangular shape of sizes $0.45 \times 0.23 \times 0.1\, mm^3$ and $1.2 \times 0.57 \times 0.2\, mm^3$ (samples Y1 and Y2, respectively). The Hall probes were made of GaAs/AlGaAs 2DEG. An array of 11 elements, with sensitivity better than $0.1\, G$, was in direct contact with the surface of the crystal, as sketched in Fig. 1. The active area of each probe was 10×10 and 30×30 μm^2 for crystals Y1 and Y2, respectively. The probes detect the component B_z of the field normal to the surface of the crystal. In the following we present data taken in the remanent state for sample Y1 at 50 K, and in the presence of 2 kG (during the increase of the field) for sample Y2 at 85 K.

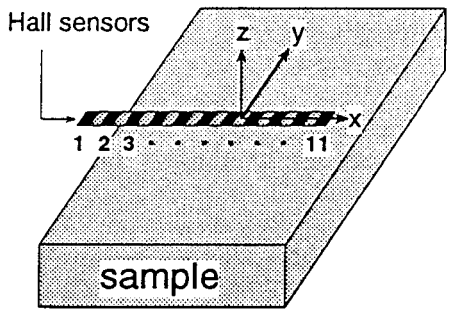

Figure 1: Configuration of Hall probe array relative to the crystal.

Figures 2a and 2b display typical field profile $B_z(x)$ across the sample width for the remanent state and in the presence of the field, for samples Y1 and Y2, respectively. Each figure shows Bean-like profiles corresponding to the indicated times; these times are measured from the moment of application (Fig. 2b) or removal of the field (Fig. 2a).

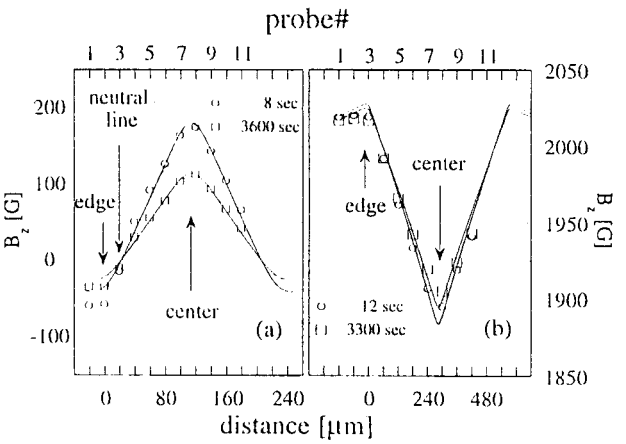

Figure 2: Local induction B_z vs. Hall probe location (a) in sample Y1 measured 8 sec and one hour after removal of the external field at $T = 50$ K and (b) in sample Y2 measured 12 sec and 3300 sec after application of a 2 kG field at $T = 85$ K. The solid lines in the figures are based on model calculation described in the Appendix.

Signatures of demagnetization effects typical for such samples[13–15] are clearly observed. Specifically, in the remanent state (Fig. 2a) a sign-reversal of B_z is observed near the edge, approximately at the location of probe #3. This point is located at the 'neutral line'[9] where vortices of different sign annihilate. Figures 3a and 3b show B_z as a function of time at different locations in the sample, for the remanent state and for field on, respectively. Evidently, the relaxation rate $\partial B_z/\partial(\ln t)$ is maximum near the center and decreases toward the edge. Moreover, in the remanent state, as a direct consequence of the sign reversal of B_z near the neutral line, the induction at the sample edge *increases* with time, exhibiting a *positive* relaxation rate. These results emphasize the non uniformity of the local relaxation, thus questioning the meaning of global measurements in which all contributions are combined. Using the raw $B_z(x,t)$ data, we calculate the local relaxation rates $\partial B_z(x,t)/\partial t$, and then numerically integrate $\partial B_z(x,t)/\partial t$ in order to determine the flux current density $D(x,t)$ according to Eq. (6):

$$D(x,t) = -\int_0^x \frac{\partial B_z(x,t)}{\partial t} dx. \tag{8}$$

In Eq. (8) $x = 0$ is the center of the sample where $D \equiv 0$.

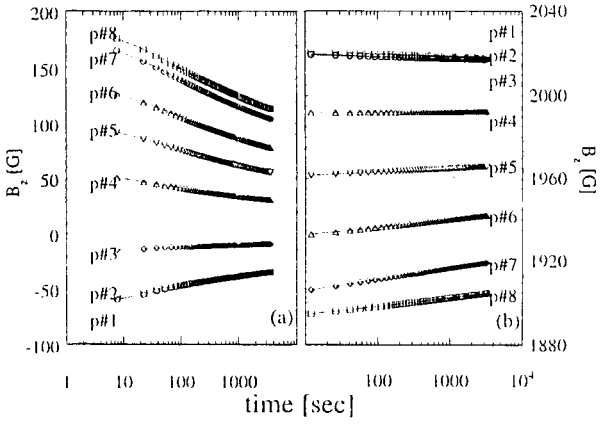

Figure 3: B_z vs. time measured at different locations in (a) sample Y1 in the remanent state at T=50 K, and (b) sample Y2 in the presence of field of 2 kG at $T = 85K$.

In Figures 4a and 4b we plot D as a function of x at different times, for the remanent state and in the presence of field, respectively. Note that a similar behavior of D, but with opposite sign, is obtained for field on and field off.

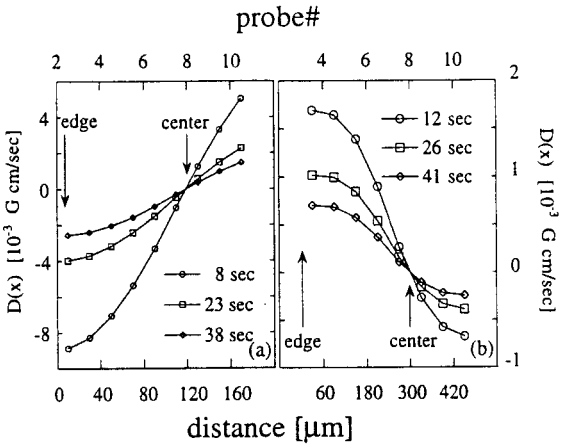

Figure 4: Flux current density D as a function of the distance from the edge, measured at the indicated times, for (a) sample Y1, (remanent state, 50 K), and (b) sample Y2 in the presence of a field (2 kG at $T = 85$ K).

This opposite sign reflects flux exit in the case of field off and flux entry in the case of field on. Note that according to equations (3) and(6) , the slope of $D(x)$ is related to the change of B_z with time. The latter is maximum at the center and it drops to zero near the edge, see Figs. 3. The behavior of D is thus consistent with this picture for both cases.

From the experimental data on the flux line current density D it is easy to derive the flux line velocity v, using the definition $D = vB_z\sqrt{1+\delta}$. The correction factor $\sqrt{1+\delta}$ is calculated as explained in the Appendix. Obviously, the correction factor is most significant in the vicinity of the neutral line in the remanent state. Typical data for v as a function of x for the remanent state and in the presence of a field are shown in Figs. 5a and 5b, respectively. The dotted line in Fig. 5a depicts $v\sqrt{1+\delta}$. Obviously, taking this correction factor into account is important near the neutral line.

It should be noted that the time dependence of v is hyperbolic; in the logarithmic approximation one obtains $v = v_0(t_0/t)$. The parameter v_0, being proportional to the current density j, depends only logarithmically on time t. Note the difference in the values of v for field on and field off. In figures 5a and 5b the velocities are of order 10^{-5} and 10^{-7} cm/sec, respectively. The lower velocity for field on can be ascribed to the higher temperature as well as to the lower field gradients.

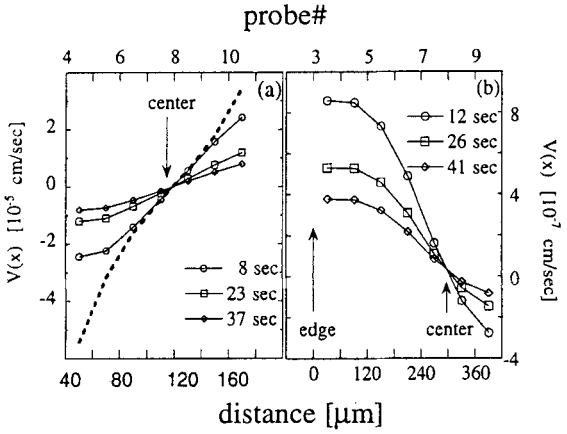

Figure 5: Flux line velocity v as a function of the distance from the edge, measured at the indicated times, for (a) sample Y1, (remanent state, 50 K), and (b) sample Y2 in the presence of a field (2 kG at $T = 85$ K). The dashed line in (a) represents the apparent velocity at $t = 8$ sec, ignoring the correction factor $\sqrt{1+\delta}$.

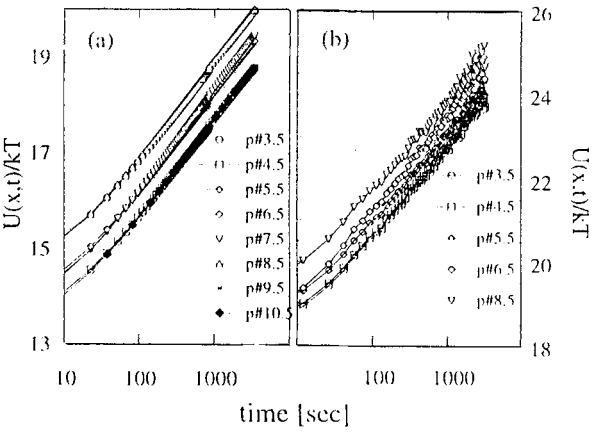

Figure 6: Local activation energy U/kT vs. time for different probes for (a) sample Y1, (remanent state, 50 K), and (b) sample Y2 in the presence of a field (2 kG at $T = 85$ K). Note that in Ref. 1, U is derived for $\delta = 0$.

Using $v(x,t)$ data, we obtain the activation energy $U(x,t)$ according to Eq. (7) as explained above. Typical results of U/kT are shown in Figures 6a and 6b as a function of time for the remanent state and in the presence of a field, respectively. The figures show a linear dependence of U/kT on $\ln(t)$ with a slope of 1 in the long-time limit in accordance with the logarithmic solution[4] of the continuity equation $U = kT\ln(t/t_0)$. The *increase* of U with time is a reflection of the increase of U with the decrease of the current density j.

4. CONCLUSIONS

We investigated the thermally activated flux creep process in YBCO crystals using a new Hall-probe array technique. We measured the time evolution of the field profiles in the sample, in the remanent state and in the presence of a field. These data were analyzed on the basis of a continuity equation for the vortex lines, taking into account the contribution of both the in-plane and the perpendicular components of the induction B. This unique approach allows a direct determination of the flux creep parameters as a function of time and position. Thus, a complete picture of the details of the relaxation process is obtained. The derived flux line current density and velocity are of opposite sign for the remanent and field-on cases, reflecting flux exit and flux entry for the two cases, respectively. Otherwise, the

behavior of the flux creep parameters is similar. Obtaining such a complete picture in one experiment is unique to our new technique. This method has the potential of giving definite answers to many open questions related to various phenomena such as collective pinning, collective creep, surface barriers, and 'fishtail' effects.[16]

We are grateful to F. Holtzberg, M. Konczykowski, A. Erb and H. Wühl for providing the crystals for this study. We thank H. Shtrikman for growing the GaAs heterostructures, and acknowledge useful discussions with M. Konczykowski, P. Kes and V. B. Geshkenbein. This work was supported by the Israel Science Foundation administered by the Israeli Academy of Science and Humanities, and the Heinrich Hertz Minerva Center for High Temperature Superconductivity. Y. Y. acknowledges support from the DG XII, Commission of the European Communities. Y. Y. and E. Z. acknowledge support from the USA-Israel Binational Science Foundation. A. S. and E. Z. acknowledge a support from the France - Israel cooperation program AFIRST. V. M. V. acknowledges support from the US Department of Energy, BES - Material Sciences, under contract no. W-31-109-ENG-38.

APPENDIX

Consider a long thin superconducting strip of rectangular cross-section of width $2w$ ($-w \le x \le w$), thickness d ($-d \le z \le 0$) and length $L >> w$. The external field H is applied along the z direction. We assume that the current density within the sample has only one component $j = (0, jsgn(x), 0)$, of a constant magnitude. The Biot-Savart law implies:

$$B_z = H + \frac{j}{c}\int_{-d}^{0} \ln\left[\frac{\left((x+w)^2+(z-z')^2\right)\left((x-w)^2+(z-z')^2\right)}{\left(x^2+(z-z')^2\right)^2}\right] dz' \equiv$$

$$\equiv H + (jd/c)G_z(x,z), \tag{9}$$

$$B_x = \frac{2j}{c}\int_{-d}^{0}\left[-2\arctan\left(\frac{x}{z-z'}\right) + \arctan\left(\frac{x+w}{z-z'}\right) + \arctan\left(\frac{x-w}{z-z'}\right)\right] dz' \equiv$$

$$\equiv (jd/c)G_x(x,z), \tag{10}$$

where $G_z(x,z)$ and $G_x(x,z)$ are dimensionless geometrical factors. In Fig. 7 we show G_x, G_z, at $z = 5\mu m$ for the ratio $w/d = 1$, which approximately corresponds to both of our crystals.

According to Eqs. (9) and (10),

$$\delta \equiv \frac{B_x^2}{B_z^2} = \frac{G_x^2}{[H/(jd/c) + G_z]^2}. \tag{11}$$

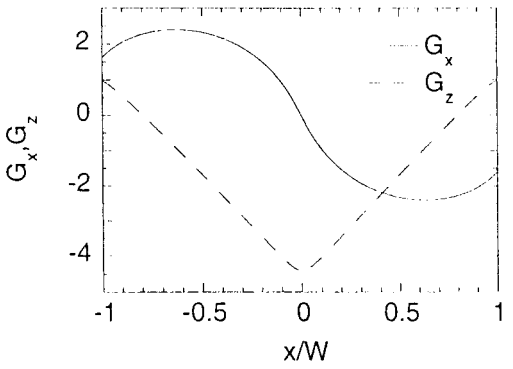

Figure 7: The geometrical factors G_x and G_z as a function of x/w at $z = 5\ \mu m$, for $w/d = 1$, corresponding approximately to samples Y1 and Y2.

For the remanent state $H = 0$ and δ is a pure geometrical factor. Fig. 8 shows the correction factor $\gamma = \sqrt{1+\delta}$ for the remanent state, calculated for different ratios $w/d = 2$, 1, and 0.25.

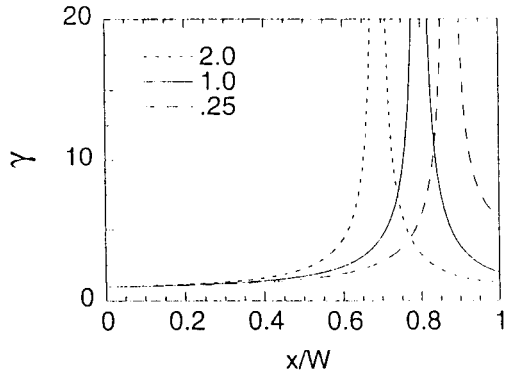

Figure 8: The correction factor $\gamma = \sqrt{1+\delta}$ as a function of x/w at $z = 5\ \mu m$, for $w/d = 2$, 1, 0.25. For samples Y1 and Y2, $w/d \approx 1$.

Evidently, the range for which the correction factor is most significant is around the neutral line, and it shifts toward the edge of the sample as

w/d decreases. Inspection of Eq. (11) shows that application of an external field suppresses the increase of δ, thus increases the range for which the correction factor is approximately 1. The correction factor in the presence of an external field can be accurately calculated in the following way: Fitting of the measured profiles of B_z to Eq. (9) yields j. This is a one parameter fit since H, G_z, and d are known. Thus, δ can be calculated using Eq. (11). Calculation of δ for sample Y2 in a field of 2 kG shows that $\delta \approx 1$ over the whole range.

REFERENCES

1. Y. Abulafia, A. Shaulov, Y. Wolfus, R. Prozorov, L. Burlachkov, Y. Yeshurun, D. Majer, E. Zeldov, and V. M. Vinokur, Phys. Rev. Lett. **75**, 2404 (1995).
2. Y. Abulafia, A. Shaulov, Y. Wolfus, R. Prozorov, L. Burlachkov, Y. Yeshurun, D. Majer, E. Zeldov, and V. M. Vinokur,, *"Coherence in High-T_c Superconductors"*, Eds. A. Revcolevschi and G. Deutscher, World Scientific Publishing (Singapore), in press.
3. M. R. Beasley, R. Labusch, and W.W. Webb, Phys. Rev. **181**, 682 (1969).
4. G. Blatter, M. V. Feigel'man, V. B. Geshkenbein, A. I. Larkin, and V. M. Vinokur, Rev. Mod. Phys. **66**, 1125 (1994).
5. Y. Yeshurun, A. P. Malozemoff, and A. Shaulov, Rev. Mod. Phys. (in press).
6. M. V. Feigel'man, V.B. Geshkenbein, and V. M. Vinokur, Phys. Rev. B **43**, 63 (1991).
7. M. P. Maley, J. O. Willis, H. Lessure, and M. E. McHenry, Phys. Rev. B **42**, 2639 (1990).
8. A. Gurevich and H. Küpfer, Phys. Rev. B **48**, 6477(1993).
9. T. Schuster, H. Kuhn, and E. H. Brandt, Phys. Rev. B **51**, 697 (1995).
10. M. Golosovsky, M. Tsindlekht, H. Chayet, and D. Davidov, Phys. Rev. B **50**, 470 (1994).
11. F. Holtzberg and C. Feild, J. Cryst. Growth **99**, 915 (1990).
12. A. Erb, T. Traulsen, and G. Muller-Vogt, J. Cryst. Growth 137, 487 (1994).
13. D. J. Frankel, J. Appl. Phys. **50**, 5402 (1979), M. Däumling and D. C. Larbalestier, Phys. Rev. B **40**, 9350 (1989).
14. E. H. Brandt, Phys. Rev. B **49**, 9024 (1994).
15. E. Zeldov, J. R. Clem, M. McElfresh, and M. Darwin, Phys. Rev. B **49**, 9802 (1994).
16. Y. Abulafia, L. Burlachkov, A. Shaulov, Y. Wolfus, R. Prozorov, Y. Yeshurun, D. Majer, E. Zeldov, H. Wühl, V. B. Geshkenbein, and V. M. Vinokur, preprint.